Journal of Catalysis **192,** 322–334 (2000)
doi:10.1006/jcat.2000.2863, available online at http://www.idealibrary.com on IDEAL®

Acetic Acid Hydrogenation over Supported Platinum Catalysts

Willy Rachmady and M. Albert Vannice

Department of Chemical Engineering, The Pennsylvania State University, University Park, Pennsylvania 16802

Received October 13, 1999; revised March 3, 2000; accepted March 3, 2000

Acetic acid was chosen to probe the kinetic behavior of carboxylic acid hydrogenation over platinum supported on TiO_2, SiO_2, η-Al_2O_3, and Fe_2O_3. The reaction was studied in the vapor phase under conditions of 423–573 K, 100–700 Torr hydrogen, and 7–50 Torr acetic acid in a differential, fixed-bed reactor. Product selectivity was strongly dependent on the oxide supports. Carbon-containing products during hydrogenation at low conversions consisted of about: 50% CO and 50% CH_4 over Pt/SiO_2; 8% ethanol, 4% ethyl acetate, 10% ethane, 40% CH_4, 33% CO, and 5% CO_2 over Pt/η-Al_2O_3; 50% ethanol, 30% ethyl acetate, and 20% ethane over Pt/TiO_2 reduced at either 473 or 773 K; and about 80% acetaldehyde and 20% ethanol over Pt/Fe_2O_3. The TiO_2-supported Pt catalysts were the most active, and both their activities and their turnover frequencies were up to two orders of magnitude larger than those for Pt dispersed on SiO_2, η-Al_2O_3, or Fe_2O_3. The activity dependence on the partial pressures of hydrogen, P_{H_2}, and acetic acid, P_A, was determined for Pt/TiO_2 catalysts at three operating temperatures—422, 445, and 465 K—after reduction at either 473 or 773 K. The apparent reaction order with respect to H_2 was found to vary between 0.4 and 0.6, while that with respect to acetic acid was between 0.2 and 0.4. One reaction model that correlated these data well involves a Langmuir–Hinshelwood-type catalytic sequence that incorporates dissociative hydrogen and acetic acid adsorption on one type of site existing on the Pt surface, but only molecular acetic acid adsorption at another type of site on the oxide surface. Only the latter species on the titania surface was considered catalytically significant in the formation of desired products, i.e., acetaldehyde, ethanol, and ethane. The resulting rate expression in terms of acetic acid disappearance has the form

$$r_{HOAc} = k_1 P_A P_{H_2}^{1/2} / \left[\left(K_2 P_{H_2}^{1/2} + K_3 P_A / P_{H_2}^{1/2} \right) (1 + K_4 P_A) \right].$$

Values of enthalpy and entropy of adsorption obtained from the optimized rate for hydrogen on platinum and acetic acid on titania were reasonable and thermodynamically consistent. © 2000 Academic Press

INTRODUCTION

The ability to synthesize industrially important chemicals, such as aldehydes, alcohols and esters, from cheap and renewable carboxylic acids is highly desirable, particularly if it can be achieved by direct hydrogenation. These reactions are particularly important for long-chain aliphatic acids. However, few quantitative studies of such reactions have been conducted. Acetic acid has been utilized as a model compound to probe both carboxylic acid adsorption and its kinetic behavior on metals, metal oxides, and supported metal catalysts because of its molecular simplicity and wide commercial application, as well as the desire to obtain a high selectivity to acetaldehyde. The patent literature describes certain catalyst systems that have been used for the production of alcohols and esters by the hydrogenation of acetic acid (1–4), and most of these catalysts are comprised of one or more Group VIII noble metals dispersed on Group III or IV metal oxides. Selectivity has been reported to vary markedly; for example, at 11 atm and temperatures near 500 K acetic acid hydrogenation over Ru/TiO_2 catalysts gave high selectivity to ethyl acetate (98% ethyl acetate, 2% ethanol) (1), whereas a Pd–Re/C reversed the selectivity and gave 93% ethanol (2). Consequently, a better understanding of the mechanistic details associated with this catalytic reaction could facilitate the design and development of better catalyst systems; unfortunately, only a few such studies have been reported in the literature. Cressely *et al.* studied acetic acid hydrogenation over Cu, Fe, or Co dispersed on an inert SiO_2 support, and their results showed that Cu/SiO_2 was active for the formation of ethanol, acetaldehyde, and ethylacetate, whereas the reaction over Fe/SiO_2 resulted in the production of acetone, and only decomposition products (CH_4, CO_2, and surface C) were obtained with Co/SiO_2 (5). These authors proposed that selective acetic acid hydrogenation to ethanol and acetaldehyde took place via adsorbed acetate intermediates, and the difference in selectivity among the three supported metal catalysts was associated with the presence or the absence of these acetate species and their relative stability.

More recently, Pestman *et al.* found that highly reducible oxides such as Fe_2O_3 and SnO_2 were active for hydrogenation of acetic acid to acetaldehyde, and this selective reaction over Fe_2O_3 was suggested to occur via a Mars—Van Krevelen-type of mechanism in which lattice oxygen and oxygen vacancies participate in the reaction (6). They also suggested that the main requirement for an active catalyst is the presence of both metallic and oxidic phases under reaction conditions. Hydrogen is activated by dissociative adsorption on the metal surface and it reacts with the active intermediate adsorbed on the oxide surface.

0021-9517/00 $35.00

In this study, we investigate the kinetic behavior of acetic acid hydrogenation over platinum dispersed on four oxide supports, TiO_2, SiO_2, η-Al_2O_3, and Fe_2O_3. Although some mechanistic details have been proposed in the literature, no reaction models have been proposed to describe the kinetics of carboxylic acid hydrogenation over supported metal catalysts. The catalytic behavior of this reaction over the catalysts mentioned above is examined, a Langmuir–Hinshelwood-type reaction sequence is proposed, and a thermodynamically consistent rate expression is presented for this reaction over Pt/TiO_2 catalysts.

EXPERIMENTAL

Catalysts were prepared using an incipient wetness technique. The four oxide supports—TiO_2 (Degussa, P25), SiO_2 (Davison, Grade 57), η-Al_2O_3 (prepared from calcining aluminum β-trihydrate), and Fe_2O_3 (Alfa Aesar, 99.95%)—were calcined at 773 K for 2 h under 100 sccm of compressed air (M.G. Industries, 99.5%) to remove any organic contaminants before impregnation with a platinum salt solution prepared by dissolving $H_2PtCl_6 \cdot 6H_2O$ (Aldrich, 99.995%) in distilled, deionized water. The metal precursor concentration was adjusted to achieve the desired total metal loading; then the solution was added dropwise to the calcined oxide support (0.6 cm^3 soln/g TiO_2, 2.2 cm^3 soln/g SiO_2, 0.5 cm^3 soln/g η-Al_2O_3, and 0.2 cm^3 soln/g Fe_2O_3), which was continuously stirred to obtain well-dispersed catalysts. The catalysts were dried in an oven at 393 K overnight in air and then stored in a desiccator. The exact metal loading was determined by atomic absorption spectroscopy and is expressed in metal weight percent.

Catalyst pretreatments, which involved reduction in flowing hydrogen at a selected temperature, were carried out *in situ* so that there was no exposure of the catalyst to air before its use for chemisorption measurements or in the reaction. The catalysts with Pt supported on SiO_2, η-Al_2O_3, and Fe_2O_3 were pretreated by heating at 2–4 K/min to 723 K under flowing H_2 (50 sccm) and then holding at this temperature for 1 h. The TiO_2-supported catalyst was subjected to two different reduction temperatures, i.e., either a low-temperature reduction (LTR) at 473 K for 2 h or a high-temperature reduction (HTR) at 773 K for 1 h. Platinum powder (Alfa Aesar, 99.999%) was also used after calcination at 673 K for 1 h under a flowing mixture of 30% O_2, 70% He followed by reduction at 723 K for 1 h.

Hydrogen chemisorption was used to determine the number of Pt surface atoms in the various supported catalysts. Experiments were carried out in a stainless steel adsorption system with a base pressure of 1×10^{-6} Torr in the cell. A more detailed description of the adsorption system is given somewhere else (7). Adsorption isotherms were recorded at 300 K over a range of 20–250 Torr using hydrogen (99.999%, M.G. Industries) which had been passed through a molecular sieve trap (Supelco) and an Oxytrap (Alltech Assoc.). Irreversible uptakes were determined by taking the difference between two consecutive isotherms separated by a 30-min evacuation at 300 K. The platinum dispersion, D, was calculated using the ratio of the total atomic hydrogen uptake to the total platinum loading, assuming a stoichiometry of unity for H_{total}/Pt_{surf}. In the cases with very small Pt crystallites, which routinely give H/Pt_{total} ratios somewhat above unity, a dispersion of unity was used. An average platinum crystallite size ($\bar{d}$) for each catalyst was then calculated using the equation

$$\bar{d}(\text{nm}) = 1.13/D. \quad [1]$$

The kinetic behavior of vapor-phase acetic acid hydrogenation was studied using a glass microreactor operated under differential conditions at atmospheric pressure. All the lines to and from the reactor were stainless steel and were heated to 373 K to prevent condensation of any reactant or products. The total conversion of acetic acid in the feed was maintained under 10% in order to minimize heat and mass transfer limitations, and this was achieved by using 50 to 100 mg catalyst and 30 sccm gas feed. Liquid acetic acid (99.7% Glacial, E.M. Science) was flashed into a stream of H_2 (99.999%, M.G. Industries) or He (99.999%, M.G. Industries) using a syringe pump (Sage Instruments) to pump the acid through a preheater maintained at 393 K upstream from the catalyst bed. A molecular sieve trap (Supelco) and an Oxytrap (Alltech Associates) were also installed in the H_2 and He lines for additional purification. The composition of the product was analyzed on-line using a Hewlett–Packard 5890 gas chromatograph equipped with a Porapak T column (Supelco). Conversion of acetic acid was determined from a carbon balance based on the analysis of compounds detected in the effluent stream, and product selectivity was based only on the carbon-containing products, which excluded the amount of water formed. The rate data were evaluated and checked using the Weisz–Prater criterion to ensure they were satisfactorily free from mass transfer limitations.

RESULTS

Hydrogen chemisorption on the unsupported and supported platinum catalysts along with the calculated dispersions and crystallite sizes are reported in Table 1. Except for the 1.91% Pt/Fe_2O_3 and Pt powder samples, the catalysts had small Pt crystallite sizes of 2.5 nm or less. The dispersion of the Pt/SiO_2 catalysts was somewhat lower than the others because an incipient wetness impregnation method was used rather than ion exchange. Catalytic activity for this reaction is defined as the rate of acetic acid (HOAc) disappearance per gram of catalyst, and the overall activity then represents hydrogenation (the formation of acetaldehyde, ethanol, and ethane), esterification,

TABLE 1

Catalyst Characterization: Hydrogen Uptakes, Dispersions, and Average Pt Crystallite Sizes

Catalysts	Total uptake (μmol H_2/g)	Irreversible uptake (μmol H_2/g)	Dispersion (H_{total}/Pt)	Pt crystallite size[b] $\bar{d}$ (nm)
0.69% Pt/TiO_2 (HTR)	3.5	2.2	0.20	(1.1)[c]
0.69% Pt/TiO_2 (LTR)	21	10.6	1.19 [1.0][a]	1.1
2.01% Pt/TiO_2 (LTR)	51	28.3	0.99	1.1
0.78% Pt/η-Al_2O_3	22	13.0	1.10 [1.0][a]	1.1
0.49% Pt/SiO_2	5.6	2.2	0.45	2.5
1.91% Pt/Fe_2O_3	1.3	0.3	0.027	—[d]
Pt powder	3.1	1.7	0.0012	940

[a] Dispersion (D) = 1 if H/Pt > 1.
[b] From $\bar{d} = 1.13/D$.
[c] Based on D of 0.69% Pt/TiO_2 (LTR).
[d] Not determined due to unusually low uptake.

ketonisation, and decomposition, which includes both decarbonylation and decarboxylation to produce CH_4, CO, and CO_2. The turnover frequency (TOF) is the activity normalized to the number of Pt surface atoms based on the measured Pt dispersion in Table 1.

Arrhenius plots of the overall activity and the hydrogenation turnover frequency for 0.69% Pt/TiO_2 (HTR), 0.69% Pt/TiO_2 (LTR), 2.01% Pt/TiO_2 (LTR), 0.78% Pt/η-Al_2O_3, 1.91% Pt/Fe_2O_3, 0.49% Pt/SiO_2, and Pt powder catalysts are shown in Figs. 1a and 1b, respectively. The kinetic data were obtained at $P_{H_2} = 700$ Torr and $P_{HOAc} = 14$ Torr under both increasing and decreasing temperature conditions in order to verify the reproducibility of the measurement and to detect if any deactivation occurred. The 0.49% Pt/SiO_2 and Pt powder catalysts are not shown in Fig. 1b because they exhibited no hydrogenation activity as defined previously.

The Pt/TiO_2 catalysts were active below 473 K while Pt supported on the other oxides did not show any activity below this temperature, and Pt powder required a much higher

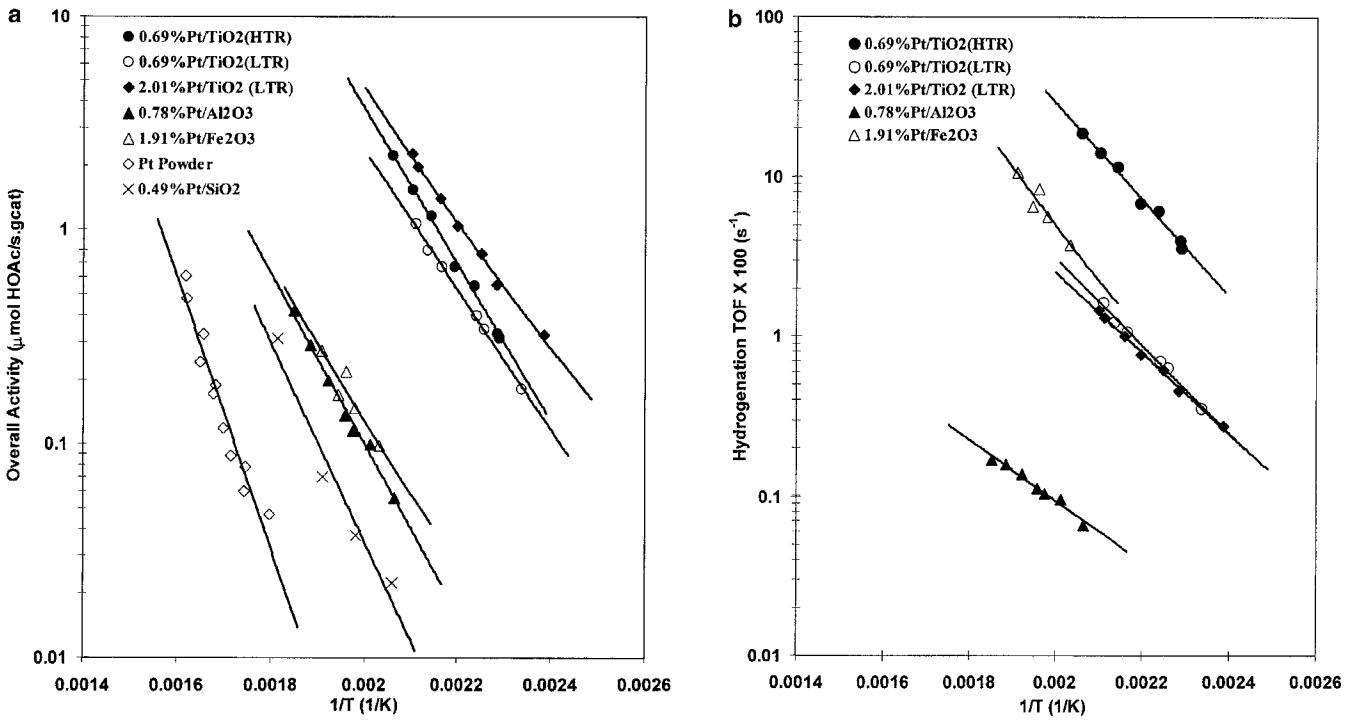

FIG. 1. Acetic acid reactivity: (a) overall activity and (b) turnover frequencies for hydrogenation over 0.69% Pt/TiO_2 (HTR), 0.69% Pt/TiO_2 (LTR), 2.01% Pt/TiO_2 (LTR), 0.78% Pt/η-Al_2O_3, and 1.91% Pt/Fe_2O_3. Reaction conditions: $P_{H_2} = 700$ Torr, $P_{HOAc} = 14.7$ Torr.

TABLE 2

Activities and Apparent Activation Energies of Hydrogenation, Esterification, Ketonisation, and Decomposition of Acetic Acid ($P_{HOAc} = 14$ Torr, $P_{H_2} = 700$ Torr)

Catalysts	Overall activity at 480 K (μmol HOAc/s · gcat)[a]	TOF at 480 K ($s^{-1} \times 100$)				Activation energy (kcal/mol)			
		Hydrogenation	Esterification	Ketonisation	Decomposition	Hydrogenation	Esterification	Ketonisation	Decomposition
0.69% Pt/TiO_2 (HTR)	1.84	15.3	7.1	0.07	2.0	13	20	29	29
0.69% Pt/TiO_2 (LTR)	1.26	2.0	1.4	0	0	13	21	—	—
2.01% Pt/TiO_2 (LTR)	2.40	1.6	0.72	0	0.13	12	20	—	24
0.78% Pt/η-Al_2O_3	0.04	0.065	0.0065	0.0020	0.052	9	7	29	23
0.49% Pt/SiO_2	0.014	0	0	0	0.13	—	—	—	21
1.91% Pt/Fe_2O_3	0.04	1.5	0	0	0	20	—	—	—
Pt powder	0.002	0	0	0	0.03	—	—	—	24
Fe_2O_3	0.004	—	—	—	—	29	—	—	—

[a] Calculated based on the overall disappearance of HOAc.

temperature of at least 573 K in order to produce observable activity. The overall activities, turnover frequencies, and apparent activation energies for hydrogenation, esterification, ketonisation, and decomposition of acetic acid over each catalyst are shown in Table 2, while product selectivity is compared at similar conversions in Table 3. For the purpose of comparison, the activities and turnover frequencies are reported at 480 K, which is close to a common temperature for all runs, and if some of the catalysts did not show any observable activity at this temperature, the values reported here are their extrapolated values. All the catalysts exhibited good activity maintenance during the first 12 h on stream, and there was no significant deactivation for any of the catalysts. Figure 2 shows representative activity maintenance behavior for the most active 0.69% Pt/TiO_2 (HTR) and (LTR) catalysts; activity loss after 2 h on stream was minimal.

In addition to being the most active, the Pt/TiO_2 catalysts were also the most selective toward the formation of ethanol and ethylacetate, as shown in Figs. 3 and 4. Both the LTR and the HTR catalysts produced over 60% ethanol at conversions near 5%; however, as the conversion and/or the temperature increased, the selectivity to ethanol decreased as that for ethylacetate, CO, CH_4, and CO_2 increased. Acetaldehyde formation, on the other hand, was quite low over both catalysts, particularly Pt/TiO_2 (LTR). Ethylacetate results from a secondary esterification reaction between ethanol and acetic acid while CO_2, CH_4, and CO are products of acetic acid decarboxylation and decarbonylation. Increasing the pretreatment reduction temperature for 0.69% Pt/TiO_2 from 473 (LTR) to 773 K (HTR) increased the activity by 45% and the turnover frequency of hydrogenation by a factor of 7, and an effect on product selectivity was demonstrated by a significant increase in CO and CH_4 formation. However, the apparent activation energies for the hydrogenation reactions were similar (13 ± 1 kcal/mol) for both the HTR and LTR catalysts. Hydrogenation activity increased as expected when the Pt loading was increased for titania-supported Pt, as shown by the results in Fig. 1 and Table 2 for 0.69% Pt/TiO_2 (LTR)

TABLE 3

Product Selectivity during Acetic Acid Hydrogenation ($P_{HOAc} = 14$ Torr, $P_{H_2} = 700$ Torr)

Catalysts	Temp. (K)	Conversion (%)	Selectivity (mol%)						
			Acetaldehyde	Ethanol	Ethane	Ester	CO_2	CO	CH_4
0.69% Pt/TiO_2 (HTR)	447	5.9	0	59	14	27	0	0	0
0.69% Pt/TiO_2 (LTR)	443	5.6	0	51	20	29	0	0	0
2.01% Pt/TiO_2 (LTR)	420	5.0	0	70	16	14	0	0	0
0.78% Pt/η-Al_2O_3	523	4.7	0	8	10	4	5	33	40
0.49% Pt/SiO_2	511	2	0	0	0	0	0	50	50
1.91% Pt/Fe_2O_3	523	4	80	20	0	0	0	0	0
Pt powder	588	4.7	0	0	0	0	32	21	47
Fe_2O_3	500	4	79	21	0	0	0	0	0

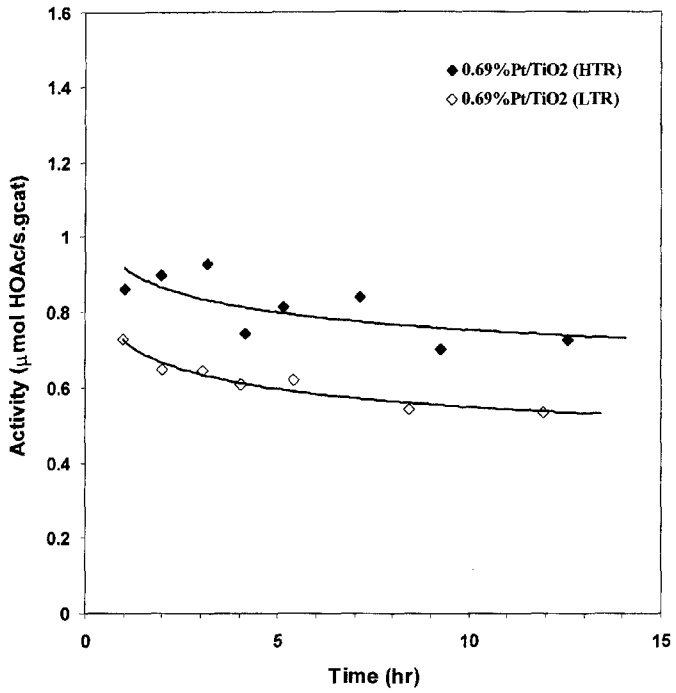

FIG. 2. Activity maintenance with 0.69% Pt/TiO_2 (HTR) and 0.69% Pt/TiO_2 (LTR). Reaction conditions: $P_{H_2} = 700$ Torr, $P_{HOAc} = 14.7$ Torr, and $T = 460$ K.

and 2.01% Pt/TiO_2 (LTR). The turnover frequency, however, remained about the same for these catalysts, indicating the expected proportionality in the kinetic regime between Pt surface atoms and the observed activity.

The products obtained with the 0.78% $Pt/\eta\text{-}Al_2O_3$ catalyst consisted primarily of CO and CH_4 with small amounts of ethanol, ethane, ethylacetate, and CO_2, as shown in Fig. 5. At 5% conversion, the product composition was about 8% ethanol, 10% ethane, 4% ethylacetate, 5% CO_2, 33% CO, and 40% CH_4. The high selectivity to CO and CH_4 was obtained because the decarbonylation reaction dominated at the temperatures required for this catalyst to be active, which were above 473 K. Compared to the hydrogenation reaction, the decarbonylation reaction is more thermodynamically favorable at higher temperatures.

The 1.91% Pt/Fe_2O_3 catalyst showed a markedly different product distribution, as it was very selective for the formation of the initial hydrogenation product, acetaldehyde (Table 3 and Fig. 6). Although activity was low and was observed only above 473 K, the turnover frequency at 480 K was slightly higher than that obtained with 0.69% Pt/TiO_2 (LTR) because with this 1.91% Pt/Fe_2O_3 catalyst, the total uptake of either hydrogen or CO was very low. Both hydrogen and CO chemisorption indicated that the Pt dispersion was only 0.006, which implies a very large Pt crystallite size of about 190 nm; however, X-ray diffraction (XRD) spectra did not indicate the presence of such large platinum particles. Therefore, an explanation other than large crystallites, such as Pt–Fe bimetallic particle formation or surface coverage of Pt by FeO_x species, appears to be more appropriate.

The 0.49% Pt/SiO_2 and Pt powder catalysts showed similar behavior, which was completely different from the other catalysts. No activity was observed below 473 K, and above this temperature only CO, CO_2, and CH_4 were observed as

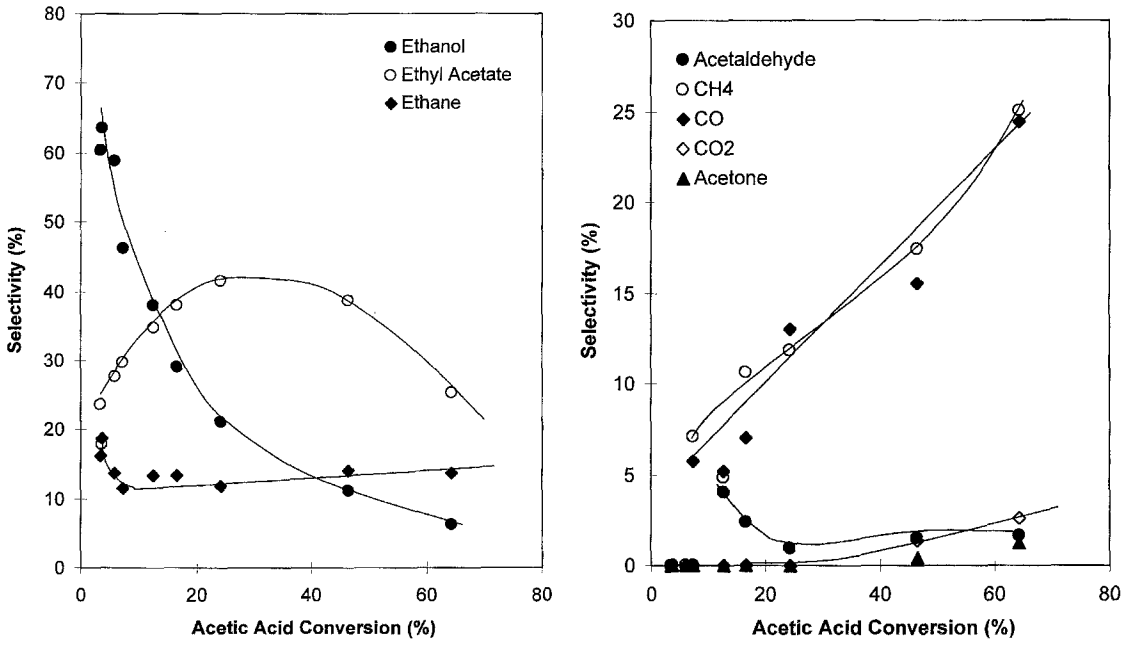

FIG. 3. Product distribution obtained from acetic acid hydrogenation over 0.69% Pt/TiO_2 (HTR). Conversion altered by varying the reaction temperature. Reaction conditions: $P_{H_2} = 700$ Torr, $P_{HOAc} = 14.7$ Torr, and $T = 423$–473 K.

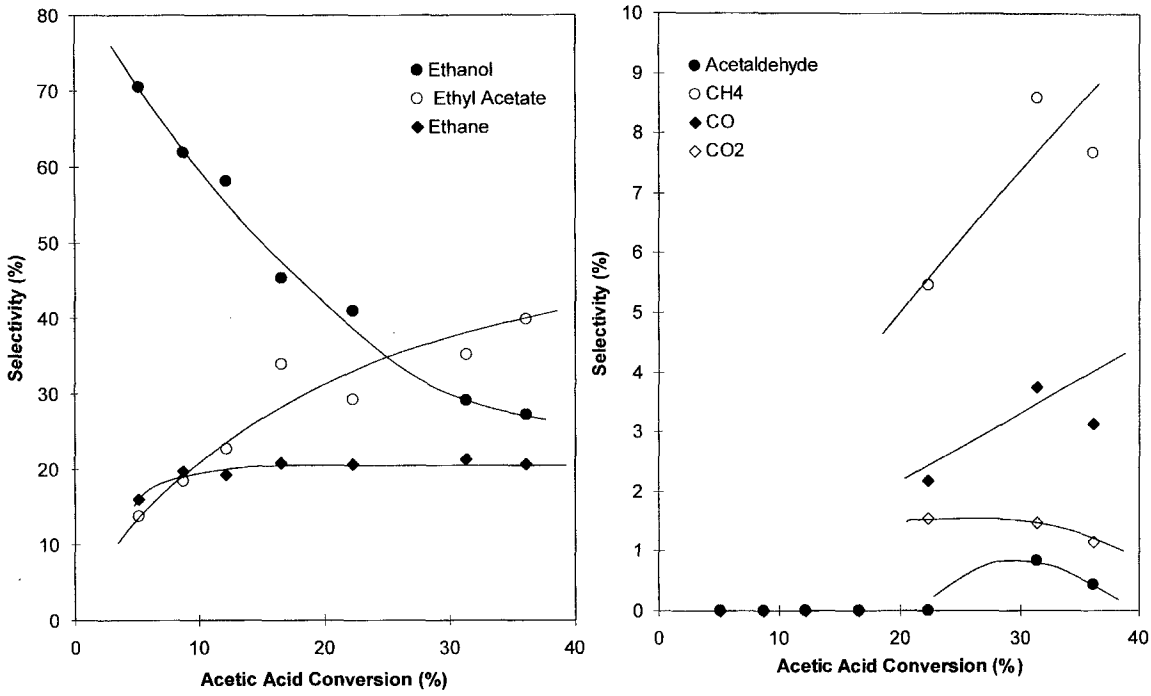

FIG. 4. Product distribution obtained from acetic acid hydrogenation over 2.01% Pt/TiO_2 (LTR). Conversion altered by varying the reaction temperature. Reaction conditions: $P_{H_2} = 700$ Torr, $P_{HOAc} = 14.7$ Torr, and $T = 423$–578 K.

products, as shown in Fig. 7. Thus only acetic acid decomposition via decarboxylation and decarbonylation reactions occurred, as verified by the molar ratios of CH_4, CO_2, and CO. The decarbonylation reaction requires the presence of hydrogen, as shown in

$$CH_3COOH + H_2 \rightarrow CH_4 + CO + H_2O \qquad [2]$$

and results in the formation of CH_4, CO, and H_2O. The

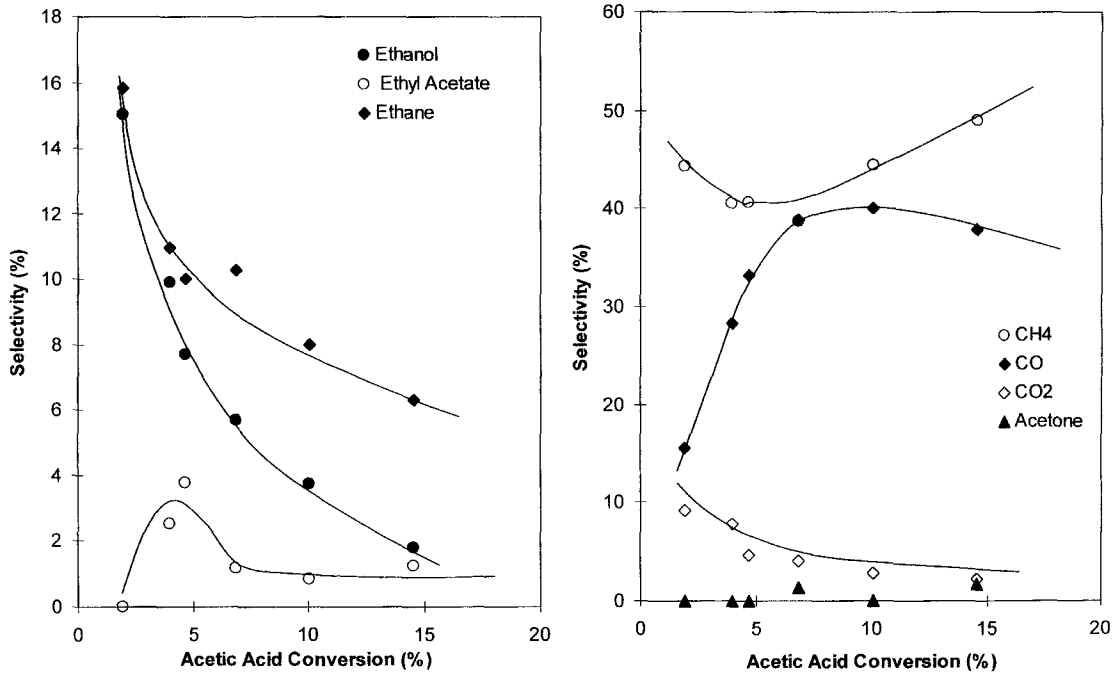

FIG. 5. Product distribution obtained from acetic acid hydrogenation over 0.78% Pt/η-Al_2O_3. Conversion altered by varying the reaction temperature. Reaction conditions: $P_{H_2} = 700$ Torr, $P_{HOAc} = 14.7$ Torr, and $T = 493$–540 K.

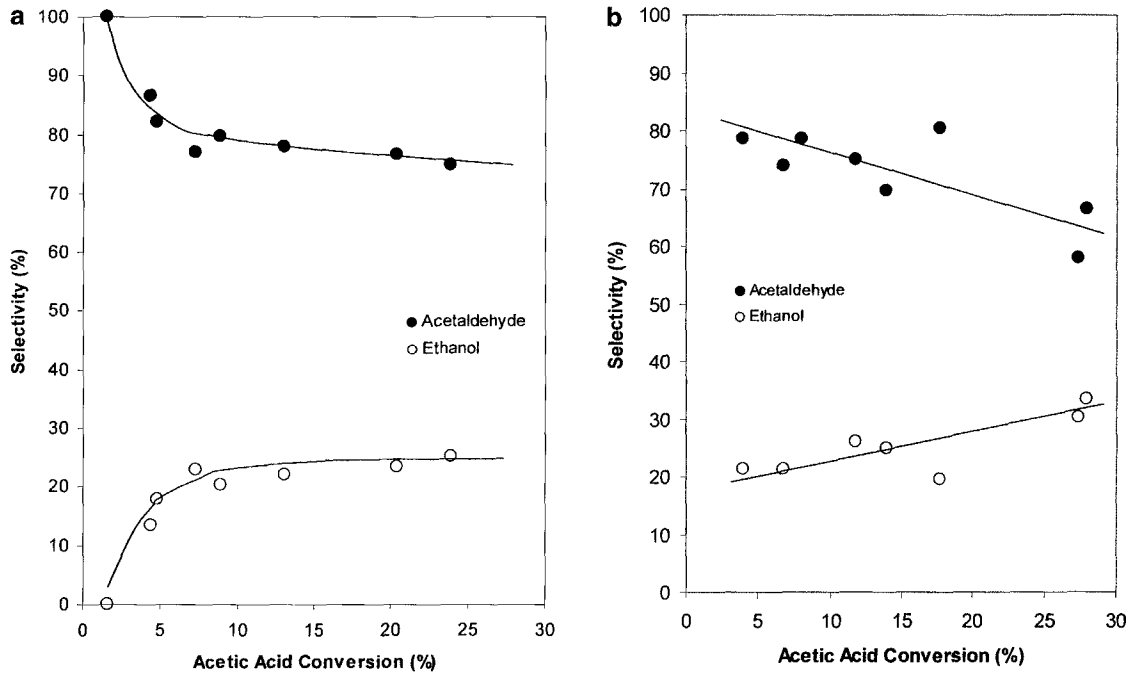

FIG. 6. Product distribution obtained from acetic acid hydrogenation over (a) 1.91% Pt/Fe_2O_3 and (b) Fe_2O_3. Conversion altered by varying the reaction temperature. Reaction conditions: $P_{H_2} = 700$ Torr, $P_{HOAc} = 14.7$ Torr, and $T = 493$–593 K.

decarboxylation reaction, however, does not require hydrogen and produces CH_4 and CO_2 as shown in

$$CH_3COOH \rightarrow CH_4 + CO_2. \quad [3]$$

Because the Pt/TiO_2 catalysts exhibited very good hydrogenation activities, both LTR and HTR samples were prepared to study the effects of reactant partial pressures on kinetic behavior. Catalytic activities were first measured at H_2 partial pressures between 100 and 700 Torr while

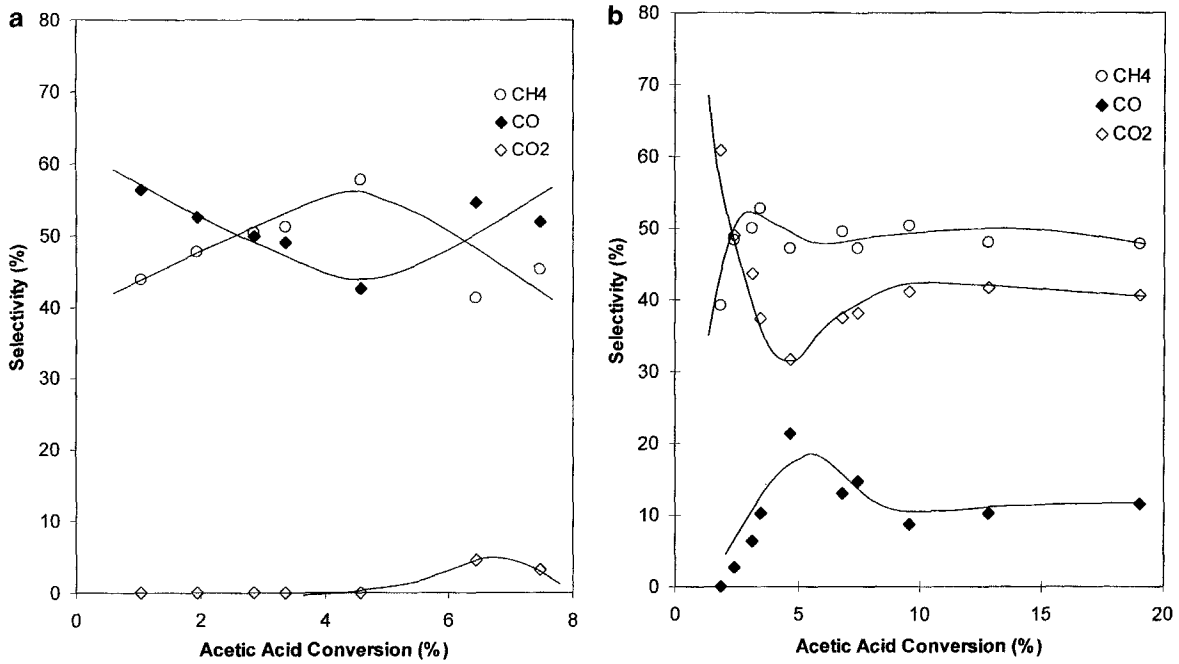

FIG. 7. Product distribution obtained from acetic acid hydrogenation over (a) 0.49% Pt/SiO_2 and (b) Pt powder. Conversion altered by varying the reaction temperature. Reaction conditions: $P_{H_2} = 700$ Torr, $P_{HOAc} = 14.7$ Torr, and $T = 485$–617 K.

acetic acid partial pressure was kept constant at 14.3 Torr, then measured at acetic acid partial pressures between 7 and 54 Torr while H_2 partial pressure was kept constant at 700 Torr. Data were obtained at three different temperatures between 422 and 473 K and, for each data set, activities were determined with both increasing and decreasing partial pressures to verify the reproducibility of the measurement. In addition, results were compared to those obtained from the separate Arrhenius run conducted at standard conditions of $P_{H_2} = 700$ Torr and $P_{HOAc} = 14.3$ Torr. The two catalysts used were 0.69% Pt/TiO_2 (HTR) and 2.01% Pt/TiO_2 (LTR), and the results showed that the apparent reaction order with respect to hydrogen varied between 0.4 and 0.6 while that with respect of acetic acid varied between 0.2 and 0.4. The apparent activation energy was found to be affected by both H_2 and acetic acid partial pressures. In the case of the 2.01% Pt/TiO_2 (LTR) catalyst, increasing the partial pressure of H_2 from 100 to 700 Torr while keeping the partial pressure of acetic acid constant at 14.3 Torr increased the activation energy from 10 to 13 kcal/mol, whereas increasing the partial pressure of acetic acid from 7 to 54 Torr while keeping the H_2 partial pressure of hydrogen constant at 700 Torr decreased the activation energy from 13 to 11 kcal/mol.

The oxide supports were also tested for activity under the standard hydrogenation reaction conditions. The SiO_2, η-Al_2O_3, and Fe_2O_3 were pretreated under flowing H_2 at 723 K for 1 h, while the TiO_2 was subjected to either an LTR or an HTR pretreatment. There was no activity detected below 473 K with these oxides; however, although SiO_2 was found to be totally inert, η-Al_2O_3, TiO_2, and Fe_2O_3 were capable of catalyzing the ketonisation reaction above 523 K, and equal amounts of acetone and CO_2 were observed. This reaction involves two acetic acid molecules, as shown in

$$2CH_3COOH \rightarrow CH_3COCH_3 + CO_2 + H_2O. \quad [4]$$

The specific activities for ketonisation on these oxides are reported in Table 4. Besides being active for ketonisation, Fe_2O_3 was also active above 523 K for hydrogenation to form acetaldehyde, but its hydrogenation activity was 10 times lower than that obtained with 1.91% Pt/Fe_2O_3.

DISCUSSION

The activity and selectivity during acetic acid hydrogenation is strongly dependent on the oxide support used, with titania-supported Pt being the most active catalyst. Platinum metal alone or the pure oxides by themselves show a marked difference in catalytic behavior under the hydrogenation conditions studied; i.e., with the exception of Pt/SiO_2, a synergism between Pt and the support clearly exists. These observations suggest either that the catalytic behavior of these supported Pt catalysts results from an interaction between the Pt crystallites and the oxide support to create new sites at the metal–support interface or that more than one type of site is required for optimal hydrogenation performance, for example, a bifunctional process involving H spillover. The former possibility can be attributed to metal–support interactions (MSI), which have been shown to exist with noble metals dispersed on TiO_2, V_2O_3, Nb_2O_5, and Ta_2O_5 (8–10). These MSI properties, in particular, have been used to explained why Ni/TiO_2 and Pt/TiO_2 are better catalysts for CO hydrogenation, compared to Ni/SiO_2 and Pt/SiO_2 (11, 12), and why a Pt/TiO_2 (HTR) catalyst can increase the specific activity for acetone hydrogenation more than 100-fold (13). Interfacial sites favoring the activation of the carbonyl bond have been proposed to explain this behavior. With respect to acetic acid hydrogenation, the influence of MSI on catalytic behavior may be less obvious; however, the activity of the HTR Pt/TiO_2 catalyst is 45% higher than that for the LTR sample, and the TOF of the former is increased more than sevenfold. The differences in selectivity were not great, although ethylacetate was favored with the HTR sample while ethanol was the principal product over the LTR Pt/TiO_2 catalyst.

Another plausible scheme for this reaction is one in which the reaction occurs because both the metallic and oxidic phases participate as active components and the kinetic behavior is dictated by the characteristics of the adsorbed species on the sites of each phase. The higher hydrogenation activity observed might be due to longer-range effects

TABLE 4

Ketonisation Activity of Individual Oxide Supports

Oxides	Surface area (m^2/g)	Activity at 523 K (μmol HOAc/s · g)	Specific activity at 523 K (μmol HOAc/s · m^2) × 10^3	App. activation energy (kcal/mol)
TiO_2 (LTR)	50	0.2	4	29
TiO_2 (HTR)	50	0.2	4	29
η-Al_2O_3	240	0.024	0.1	33
SiO_2	220	0	0	n.a.
Fe_2O_3	8	0.04	5	29

involving hydrogen spillover from Pt atoms to acetic acid molecules adsorbed on the oxide surface. A similar model has been used to describe the kinetics of hydrogenation of aromatics on supported Rh catalysts (14) and hydrogenation of toluene and benzene on supported Pt catalysts (15, 16).

Platinum supported on different oxides but with similar Pt dispersion, i.e., 0.69% Pt/TiO_2 (LTR), 0.49% Pt/SiO_2, and 0.78% Pt/η-Al_2O_3, did not show similar activity and selectivity. This illustrates the importance of the oxide phase in these reaction kinetics because the crystallite sizes are small and comparable, and the variation in product selectivity must be associated with the nature of acetic acid adsorption on these different oxide surfaces. Only the TiO_2- and η-Al_2O_3-supported catalysts yielded ethanol and acetaldehyde during acetic acid hydrogenation, while the Pt/SiO_2 catalyst was active only for decarbonylation to produce CH_4 and CO (and H_2O). The similarity in selectivity between Pt powder and Pt/SiO_2 indicates that the acetic acid decarbonylation reaction takes place on the Pt surface, a conclusion further supported by the fact that SiO_2 is completely inert under the reaction conditions considered (see Table 4).

It appears there is a correlation between good hydrogenation catalysts and oxides that are active for ketonisation in that the former contain the latter as a support. If acetic acid reactions on the oxides in the absence of Pt are considered, SiO_2 is not active, whereas TiO_2 and Fe_2O_3 have similar specific activities at 523 K, as indicated in Table 4. However, under the hydrogenation conditions used here, ketonisation is suppressed almost completely and hydrogenation dominates when Pt is dispersed on the oxides. These results suggest that ketonisation and hydrogenation involve the same surface intermediate and that activity and selectivity are dictated by the adsorption behavior of acetic acid on these oxide surfaces as well as the availability of activated hydrogen, presumably in the form of atomic hydrogen. The role of Pt is to provide this activated hydrogen, which can react with surface species on the oxide support to form acetaldehyde, ethanol, and ethane (17, 18). Hydrogenation may be favored over ketonisation in the presence of activated hydrogen because the ketonisation reaction has a higher activation energy of 29–33 kcal/mol compared to values of 9–23 kcal/mol for hydrogenation. The possibility that H atoms may migrate and block certain adsorption sites on the oxide support cannot be discounted, however.

Different behavior was obtained with the 1.91% Pt/Fe_2O_3 catalyst. Fe_2O_3 by itself shows selectivity similar to that with the Pt/Fe_2O_3 catalyst, as shown in Table 2. This is not surprising because, as reported by Pestman *et al.*, Fe_2O_3 contains Fe^0 and Fe_3O_4 after reduction at 723 K for 1 h (18). Dispersing Pt on this oxide increases the activity presumably because reduction of Fe_2O_3 is enhanced by the Pt, and, in addition, Pt increases the concentration of activated hydrogen under reaction conditions. Thus the activity per gram catalyst of Pt/Fe_2O_3 was almost 10 times higher than that of Fe_2O_3 alone. The selectivity obtained with Pt/TiO_2, Pt/η-Al_2O_3, and Pt/Fe_2O_3 can be dependent on conversion and temperature, as well as the nature of the active sites; for example, high conversion would further facilitate secondary reactions and higher temperatures would affect equilibrium adsorption constants for reactants, as well as altering rate constants. The different selectivity behavior among Pt/TiO_2, Pt/η-Al_2O_3, and Pt/Fe_2O_3 could be simply a consequence of different adsorption strengths of reactants and products on these catalysts. Assuming acetaldehyde is the first product of acetic acid hydrogenation, further hydrogenation to ethanol, or other secondary products such as ethylacetate, is very much dependent on the adsorption strength of acetaldehyde as well as its rate of hydrogenation. A large adsorption equilibrium constant would result in a high surface concentration of acetaldehyde, and would thus favor further hydrogenation to ethanol. The much higher acetaldehyde selectivity of Pt/Fe_2O_3 implies a much lower surface coverage of acetaldehyde due to a much higher rate of desorption on this catalyst during competitive adsorption compared to Pt/TiO_2. In addition, on the latter catalyst, the TOF for acetaldehyde hydrogenation is 1000-fold higher than that for acetic acid (19). The significant formation of ethylacetate over Pt/TiO_2 is the result of a secondary reaction between acetic acid and ethanol. As expected, the formation of this compound is pronounced at high acetic acid conversions and is minimal on Pt/Fe_2O_3 since little ethanol is formed on this catalyst. The low selectivity to hydrogenation products with Pt/η-Al_2O_3 appears to be due to a low hydrogenation rate constant because the hydrogenation turnover frequency on this catalyst is one order of magnitude lower than that on the Pt/TiO_2 catalysts, whereas the decomposition turnover frequencies are comparable.

The following important observations can be made about the kinetic behavior of acetic acid hydrogenation to form organic compounds over supported Pt catalysts:

1. The reaction requires both metal and an appropriate oxide phase in the catalyst.
2. Oxides that are active for ketonisation are the best supports, implying the reaction can occur on the oxide surface.
3. The metal, in this case Pt, acts as a source of activated hydrogen, presumably hydrogen atoms.
4. For Pt/TiO_2 the reaction orders varied between 0.2 and 0.4 with respect to acetic acid and between 0.4 amd 0.6 with respect to hydrogen.
5. The apparent activation energy is affected by both H_2 and acetic acid partial pressures.

Based on the above statements, various reaction models were considered for the hydrogenation of acetic acid to form acetaldehyde, ethanol, and ethane over Pt/TiO_2

catalysts, and a Langmuir–Hinshelwood-type catalytic sequence provided a derived rate expression that gave the most consistent fit of the data (19). Hydrogen and acetic acid were assumed to adsorb dissociatively on one type of site existing on the metal surface in quasi-equilibrated processes. It is well known that hydrogen adsorbs dissociatively on clean Pt surfaces, and hydrogen spillover, i.e., the migration of H atoms from the metal to the oxide surface, is a well-known phenomenon (20). Vajo *et al.* have shown that acetic acid adsorbs dissociatively on polycrystalline Pt surfaces to form a surface acetate species (21), and this surface acetate can recombine with a hydrogen atom and desorb as an acetic acid molecule. These processes are represented by Eqs. [5–7] in the reaction sequence, where * represents an active site on the Pt surface. The CH_3COO^* species was assumed to be stable at low temperatures, but at higher temperatures it can decompose to give CH_3 and CO_2 or, under a hydrogen atmosphere, it can undergo decarbonylation to form CH_4, CO, and H_2O, as indicated by the selectivity behavior of Pt powder. The adsorption of hydrogen and acetic acid on these Pt sites is considered to be quasi-equilibrated, with adsorbed hydrogen atoms (H^*) and acetate (CH_3COO^*) species assumed to be the abundant surface intermediates. In addition, acetic acid also can adsorb at sites on the oxide surface. Kim and Barteau have reported that acetic acid adsorbs reversibly on titania (anatase) as both weakly bound molecular acetic acid and a strongly adsorbed surface acetate species (22). These authors also found that during TPD this acetate species decomposed at 615 K into ketene, acetone, and carbon dioxide along with small amounts of methane, ethylene, carbon monoxide, and hydrogen. Under a hydrogen environment, it is assumed that weakly adsorbed molecular acetic acid is the active intermediate in the hydrogenation reaction, and acetic acid adsorption on the support is also assumed to be quasi-equilibrated, as depicted in Eq. [8] in the sequence, where S is a site on the oxide surface.

This adsorbed species is then involved in a series of irreversible surface reactions consisting of the consecutive addition of adsorbed hydrogen atoms to an adsorbed acetic acid molecule. Acetaldehyde is formed as the first initial product, and it can either desorb or react with additional hydrogen atoms to form ethanol and, subsequently, ethane. These surface reactions and reversible desorption steps are depicted by Eqs. [9]–[17] in the following sequence of elementary steps:

$$H_{2(g)} + 2^* \overset{K_{H_2}}{\Leftrightarrow} 2H^* \quad [5]$$

$$H^* \overset{K_{sp}}{\Leftrightarrow} H_{sp} \quad [6]$$

$$CH_3COOH_{(g)} + 2^* \overset{K_{Ac}}{\Leftrightarrow} CH_3COO^* + H^* \quad [7]$$

$$CH_3COOH_{(g)} + S \overset{K_A}{\Leftrightarrow} CH_3COOH\text{-}S \quad [8]$$

$$CH_3COOH\text{-}S + H_{sp} \xrightarrow{k_1} CH_3COOH_2\text{-}S \quad [9]$$

$$CH_3COOH_2\text{-}S + H_{sp} \xrightarrow{k_2} CH_3CHO\text{-}S + H_2O_{(g)} \quad [10]$$

$$CH_3CHO\text{-}S \underset{k_{-3}}{\overset{k_3}{\rightleftharpoons}} CH_3CHO_{(g)} + S \quad [11]$$

$$CH_3CHO\text{-}S + H_{sp} \xrightarrow{k_4} CH_3CHOH\text{-}S \quad [12]$$

$$CH_3CHOH\text{-}S + H_{sp} \xrightarrow{k_5} CH_3CH_2OH\text{-}S \quad [13]$$

$$CH_3CH_2OH\text{-}S \underset{k_{-6}}{\overset{k_6}{\rightleftharpoons}} CH_3CH_2OH_{(g)} + S \quad [14]$$

$$CH_3CH_2OH\text{-}S + H_{sp} \xrightarrow{k_7} CH_3CH_2OH_2\text{-}S \quad [15]$$

$$CH_3CH_2OH_2\text{-}S + H_{sp} \xrightarrow{k_8} CH_3CH_3\text{-}S + H_2O_{(g)} \quad [16]$$

$$CH_3CH_3\text{-}S \underset{k_{-9}}{\overset{k_9}{\rightleftharpoons}} CH_3CH_{3(g)} + S. \quad [17]$$

The hydrogenation activity is determined by the rate of acetic acid disappearance to form hydrogenated products, i.e., the overall rate of formation of acetaldehyde, ethanol, and ethane, as shown in Eq. [18]:

$$r_{HOAc} = r_{acetaldehyde} + r_{ethanol} + r_{ethane}. \quad [18]$$

It follows from Eqs. [11], [14], and [17] that the rates of formation of these products can be expressed as

$$r_{acetaldehyde} = k_3\theta_{acetaldehyde} - k_{-3}P_{acetaldehyde}\theta_S \quad [19]$$

$$r_{ethanol} = k_6\theta_{ethanol} - k_{-6}P_{ethanol}\theta_S \quad [20]$$

$$r_{ethane} = k_9\theta_{ethane} - k_{-9}P_{ethane}\theta_S, \quad [21]$$

where θ_i is the fractional surface coverage of species i, with S representing an empty site, and P_i is the partial pressure of species i. Applying the steady-state approximation to the surface intermediates, it can be easily shown that

$$r_{HOAc} = k_1\theta_A C_H, \quad [22]$$

where the subscript A refers to the acetic acid molecules adsorbed on the oxide and C_H is the concentration of hydrogen atoms at this site on the oxide surface. The total number of active sites is incorporated in k_1.

The quasi-equilibrium expressions representing adsorption on the Pt surface are

$$K_{H_2} = \theta_H^2/P_{H_2}\theta_*^2 \quad [23]$$

$$K_{Ac} = \theta_{Ac}\theta_H/P_A\theta_*^2, \quad [24]$$

where subscripts * and Ac, represent vacant sites and acetate on the Pt surface, respectively. The quasi-equilibrium expressions for acetic acid adsorption and H atom concentration at the oxide surface site are written as

$$K_A = \theta_A/P_A\theta_S \quad [25]$$

$$K_{sp} = C_H/\theta_H. \quad [26]$$

Expressions for θ_A and C_H can be obtained from Eqs. [23]–[26], and substitution into Eq. [22] gives

$$r_{HOAc} = k_1 K_A K_{sp} K_{H_2}^{1/2} P_A P_{H_2}^{1/2} \theta_S \theta_*, \quad [27]$$

where k_1 includes the active site concentration.

Because adsorbed hydrogen atoms (H*) and adsorbed acetate species (CH_3COO^*) are the predominant surface species on Pt, a balance on * sites gives the expression for θ_*

$$\theta_* = \frac{1}{\left(K_{H_2}^{1/2} P_{H_2}^{1/2} + K_{Ac} P_A / K_{H_2}^{1/2} P_{H_2}^{1/2}\right)}, \quad [28]$$

and if the reaction runs at low conversion so that product concentrations are low, it can be assumed that molecular acetic acid is the only significant surface intermediate on the oxide surface sites, which gives

$$\theta_S = \frac{1}{(1 + K_A P_A)}. \quad [29]$$

The final rate expression is obtained by substituting Eqs. [28] and [29] into Eq. [27] to give

$$r_{HOAc} = \frac{k_1 K_A K_{sp} K_{H_2}^{1/2} P_A P_{H_2}^{1/2}}{\left(K_{H_2}^{1/2} P_{H_2}^{1/2} + K_{AC} P_A / K_{H_2}^{1/2} P_{H_2}^{1/2}\right)(1 + K_A P_A)}$$

$$= \frac{k_1' P_A P_{H_2}^{1/2}}{\left(K_2 P_{H_2}^{1/2} + K_3 P_A / P_{H_2}^{1/2}\right)(1 + K_4 P_A)} \quad [30]$$

where $k_1' = k_1 K_A K_{sp} K_{H_2}^{1/2}$, $K_2 = K_{H_2}^{1/2}$, $K_3 = K_{Ac}/K_{H_2}^{1/2}$, and $K_4 = K_A$.

This equation was fitted to the experimental data obtained from the Arrhenius and the partial pressure runs with the 0.69% Pt/TiO_2 (HTR) and 2.01% Pt/TiO_2 (LTR) catalysts using a least-squares nonlinear optimization method. The iteration process was initiated with a number of sets of initial values, each with initial reasonable values for k_1', K_2, K_3, and K_4, and it continued until optimum values were obtained. The rate expression represented by Eq. [30] was fitted to the experimental data at three temperatures to obtain three separate values for k_1', K_2, K_3, and K_4 (Table 5), and the results using these optimized parameters are shown in Figs. 8 and 9. This expression fits all the data satisfactorily, and there was excellent agreement between the experimental and the predicted values for the apparent activation energies. Recalling that the equilibrium adsorption constants can be written as

$$K_{ad,i} = \exp\left(\Delta S_{ad,i}^0/R - \Delta H_{ad,i}^0/RT\right), \quad [31]$$

where R is the ideal gas law constant, T is temperature, and $\Delta S_{ad,i}^0$ and $\Delta H_{ad,i}^0$ are the standard entropy and enthalpy of adsorption, respectively, for compound i, one can obtain ΔS_{ad}^0 and ΔH_{ad}^0 for H_2 and acetic acid by plotting

TABLE 5

Optimized Rate Parameters in Equation [30] for Pt/TiO_2 Catalysts

Catalysts	k_1K_{sp} (μmol/s·gcat)	K_{H_2} ($atm^{-1} \times 10^{-5}$)	K_A (atm^{-1})	K_{Ac} ($atm^{-1} \times 10^{-7}$)
A. 0.69% Pt/TiO_2 (HTR)				
Temp. (K) = 437	2.42	50.8	10.9	13.5
Temp. (K) = 460	17.9	7.6	4.4	4.7
Temp. (K) = 470	22.2	4.8	5.5	3.3
B. 2.01% Pt/TiO_2 (LTR)				
Temp. (K) = 422	8.16	17.4	4.3	8.9
Temp. (K) = 445	26.6	6.1	3.3	4.2
Temp. (K) = 465	627	0.7	0.4	0.9

ln K_2^2, ln K_2K_3, and ln K_4 versus $1/T$, and their values are reported in Table 6. Both the enthalpies and entropies are expected to be negative, and evaluation criteria show them to be reasonable and thermodynamically consistent (23, 24). The enthalpy values for H_2 on TiO_2-supported Pt are fairly high compared to integral ΔH_{ad}^0 values determined calorimetrically for irreversible adsorption, but they are similar to initial heats of adsorption on clean, single-crystal Pt surfaces (25). This could imply that the values measured kinetically correspond only to H atoms adsorbed on the high-energy sites present at low H coverages.

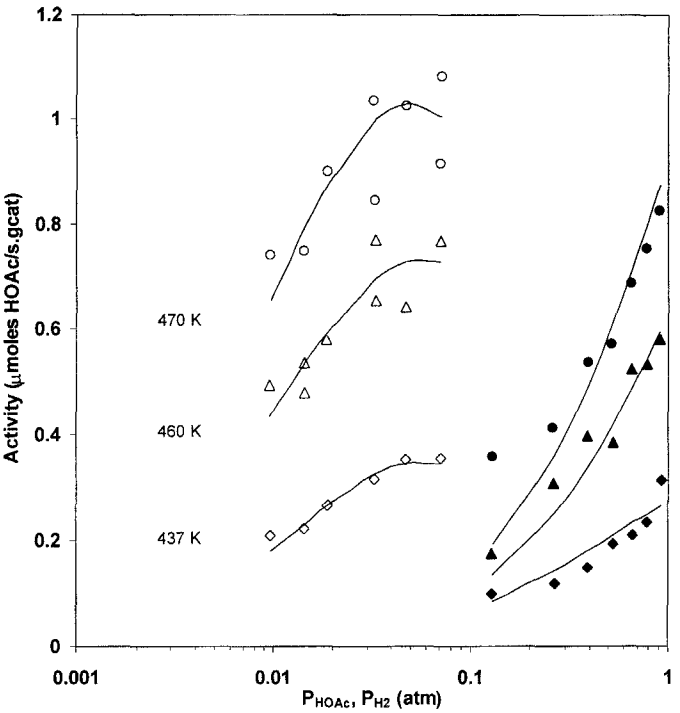

FIG. 8. Hydrogenation activity over 0.69% Pt/TiO_2 (HTR) at 437, 460, and 470 K versus acetic acid and hydrogen partial pressures. Solid lines indicate the optimum fit obtained by fitting Eq. [30] to the experimental data points.

TABLE 6

Enthalpies and Entropies of Adsorption from Rate Parameters (Standard State: 1 atm)

	Acetic acid on TiO_2		Hydrogen on Pt		Acetic acid on Pt	
Catalyst	ΔH^0_A (kcal/mol)	ΔS^0_A (cal/mol · K)	$\Delta H^0_{H_2}$ (kcal/mol)	$\Delta S^0_{H_2}$ (cal/mol · K)	ΔH^0_{Ac} (kcal/mol)	ΔS^0_{Ac} (cal/mol · K)
0.69% Pt/TiO_2 (HTR)	−10	−18	−29	−38	−32	−22
2.01% Pt/TiO_2 (LTR)	−22	−47	−29	−39	−35	−31

This interpretation is consistent with the fact that this reaction takes place at higher temperatures (above 423 K) than many other hydrogenation reactions. The enthalpies for nondissociative acetic acid adsorption on TiO_2 surfaces are not high, and they indicate bonding is stronger on the LTR TiO_2 surface, which should have more hydroxyl groups and fewer oxygen vacancies than the HTR surface (10, 26–28). Acetic acid is known to adsorb molecularly on oxide surfaces, and the reaction model forwarded here proposes that an adsorbed acetic acid molecule is the catalytically significant species. Carboxylate ions, acyl carbonium ions, and ketenes may form, but these H-deficient species, relative to acetic acid, do not participate in the formation of acetaldehyde, ethanol, or ethane. Overall, the model presented here demonstrates that acetic acid hydrogenation over titania-supported platinum catalysts can be satisfactorily described by a Langmuir–Hinshelwood-type reaction mechanism. Even if all the active sites on the TiO_2 surface exist only in the metal–support interfacial region, as proposed for other reactions involving carbonyl bonds (29), this reaction model is still applicable; the only difference is that the H spillover distance is very short.

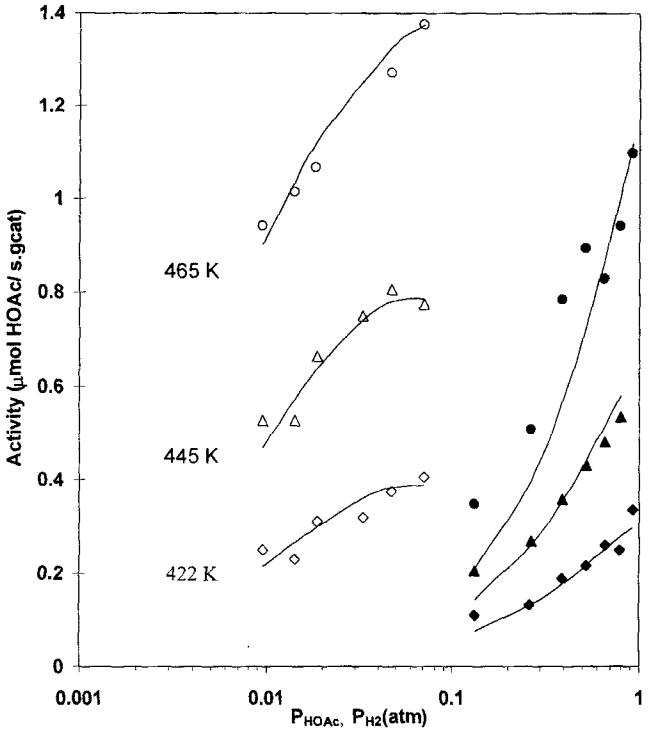

FIG. 9. Hydrogenation activity over 2.01% Pt/TiO_2 (LTR) at 422, 445, and 465 K versus acetic acid and hydrogen partial pressures. Solid lines indicate the optimum fit obtained by fitting Eq. [30] to the experimental data points.

SUMMARY

The catalytic behavior of acetic acid hydrogenation over Pt supported on TiO_2, SiO_2, η-Al_2O_3, and Fe_2O_3 was investigated. Strong evidence was obtained that the reaction involves both metal (Pt) and oxide support, and it takes place at sites on the oxide surface. Thus, the interaction of acetic acid with the oxide support plays a major role in determining the kinetics of the reaction, and the principal role of Pt in this case is to serve as a source of mobile, activated hydrogen atoms. Pt/TiO_2 catalysts were the most active for acetic acid hydrogenation, with the HTR sample having a TOF 7–8 times greater than the LTR catalyst and more than 100-fold times higher than the other Pt catalysts, and Pt/TiO_2 gave the highest selectivity to ethanol (up to 70%). A Pt/Fe_2O_3 catalyst was also active for hydrogenation, and gave a particularly high selectivity to acetaldehyde, i.e., 80% acetaldehyde and 20% ethanol, but it required a much higher temperature of operation than Pt/TiO_2. In contrast, decarbonylation and decomposition reactions dominated on Pt powder, Pt/SiO_2, and Pt/η-Al_2O_3. This study provides evidence that acetic acid hydrogenation over supported Pt catalysts can be described by a Langmuir–Hinshelwood-type mechanism invoking two types of sites, one on the metal to activate H_2 and one on the oxide to molecularly adsorb acetic acid, and the kinetic rate expression derived from this reaction model fits the data well with thermodynamically consistent parameters.

ACKNOWLEDGMENTS

This study was sponsored by the DOE, Division of Basic Energy Sciences, via Grant DE-FO2-84ER13276. We thank Utpal Singh for preparing the Pt/SiO_2 catalyst and Deepak D. Poondi for preparing the Pt/Al_2O_3 catalyst.

REFERENCES

1. Pimblett, G., Mclachlan, K. A., and Price, P. J., European Patent Application 0.372.847.A2 (1989).
2. Kitson, M., and Williams, P. S., European Patent Application 0.198.681.A2 (1986).
3. Kitson, M., and Williams, P. S., European Patent Application 0.198.682.A2 (1986).
4. Kitson, M., and Williams, P. S., European Patent Application 0.285.420.A2 (1986).
5. Cressely, J., Farkhani, D., Deluzarche, A., and Kiennemann, A., *Mater. Chem. Phys.* **11**, 413 (1984).
6. Pestman, R., Pieterse, J. A. Z., and Ponec, V., *J. Catal.* **168**, 255 (1995).
7. Chen, A., Kaminsky, M., Geoffroy, G. L., and Vannice, M. A., *J. Phys. Chem.* **90**, 4810 (1986).
8. Baker, R. T. K., Prestridge, E. B., and Garten, R. L., *J. Catal.* **56**, 390 (1979).
9. Tauster, S. J., and Fung, S. C., *J. Catal.* **55**, 29 (1978).
10. Resasco, D. E., and Haller, G. L., *Adv. Catal.* **36**, 173 (1989).
11. Burch, R., and Flambard, A. R., *J. Catal.* **85**, 16 (1984).
12. Vannice, M. A., and Twu, C. C., *J. Catal.* **82**, 213 (1983).
13. Sen, B., and Vannice, M. A., *J. Catal.* **113**, 52 (1988).
14. Ioannides, I., and Verykios, X. E., *J. Catal.* **143**, 175 (1993).
15. Lin, S. D., and Vannice, M. A., *J. Catal.* **143**, 554 (1993).
16. Lin, S. D., and Vannice, M. A., *J. Catal.* **143**, 563 (1993).
17. Pestman, R., Ph.D. Thesis, Leiden, The Netherlands, 1995.
18. Pestman, R., Koster, R. M., Boellard, E., van der Kraan, A. M., and Ponec, V., *J. Catal.* **174**, 142 (1998).
19. Rachmady, W., Ph.D. Thesis, Pennsylvania State University, in progress.
20. Pajonk, G. M., *in* "Handbook of Heterogeneous Catalysis" (G. Ertl, H. Knozinger, and J. Weitkamp, Eds.), Vol. 3, p. 1064. Wiley-Verlag Chemie, Weinheim, 1997.
21. Vajo, J. J., Sun, Y.-K., and Weinberg, W. H., *Appl. Surf. Sci.* **29**, 165 (1987).
22. Kim, K. S., and Barteau, M. A., *Langmuir* **4**, 945 (1988).
23. Boudart, M., *AIChE J.* **18**, 465 (1972).
24. Vannice, M. A., Hyun, S. H., Kalpacki, B., and Liauh, W. C., *J. Catal.* **56**, 358 (1979).
25. Sen, B., Chou, P., and Vannice, M. A., *J. Catal.* **101**, 517 (1986).
26. Lu, G., Linsebigler, A., and Yates, J. T., Jr., *J. Phys. Chem.* **98**, 11733 (1994).
27. Huizinga, T., and Prins, R., *J. Phys. Chem.* **85**, 2156 (1981).
28. Goodenough, J. B., *in* "Prog. in Solid State Chemistry" (H. Reiss, Ed.), Chap. 4. Pergamon, New York, 1971.
29. Vannice, M. A., *Topics Catal.* **4**, 241 (1997).